Available online at www.sciencedirect.com
ScienceDirect
Journal of Sound and Vibration 312 (2008) 354–359
JOURNAL OF SOUND AND VIBRATION
www.elsevier.com/locate/jsvi

Short Communication

An asymptotic solution of the governing equation for the natural frequencies of a cantilevered, coupled beam model

Harry E. Williams

Harvey Mudd College, Claremont, CA 91711, USA

Received 26 April 2006; received in revised form 28 September 2007; accepted 16 October 2007

Abstract

An asymptotic solution is presented for the natural frequencies, mode shapes of a cantilevered, coupled beam model. A three-term expansion is obtained for the frequency, which shows good agreement with exact values over a wide range of the stiffness parameter α. The first three mode shapes are also presented for large α, and show good agreement for the first and second modes. Agreement for the third mode improves as α gets larger. The modeled structure behaves essentially as a shear beam except in the immediate neighborhood of the ends.

1. Introduction

The following equation was proposed by Miranda and Taghavi [1] to describe the transverse mode of a uniform, coupled beam model:

$$\phi^{iv}(x) - \alpha^2\phi''(x) - (\rho\omega^2 L^4/EI)\phi = 0. \tag{1}$$

The mass per unit length is ρ, the length (height) is L and EI is the flexural rigidity. The natural frequency is ω, the parameter $\alpha^2 = \mathrm{GA}L^2/EI$ and GA is the shear rigidity. The solution of Eq. (1) for a cantilever ($0 \leqslant X \leqslant L$, $x = X/L$) is subject to the following boundary conditions:

$$\phi(x=0) = 0, \quad \phi'(x=0) = 0, \quad \phi''(x=1) = 0, \quad \phi'''(x=1) - \alpha^2\phi'(x=1) = 0. \tag{2}$$

This equation was originally proposed by Heidebrecht and Smith [2] as a model for shear wall-frame buildings.

Exact solutions of Eq. (1) for arbitrary α have been presented in Refs. [1,2]. However, for large values of the parameter α, calculations are difficult due to the appearance of exponentially large terms. In order to address this difficulty, we propose an approximate solution of Eq. (1) for $\alpha \gg 1$ obtained by the method of matched asymptotic expansions as proposed by Kevorkian and Cole [3]. This method has been used previously [4] by the author to analyze the transverse vibrations of a beam string. The current study was motivated by the observation that the coupled beam model and the beam string are governed by the same differential equation.

E-mail address: Harry_Williams@hmc.edu

0022-460X/$ - see front matter
doi:10.1016/j.jsv.2007.10.048

It should also be noted that this analogy was observed earlier by Traum and Zalewski [5] in the case of static loading.

As a preliminary, let us define the small parameter $\varepsilon = 1/\alpha$, and rewrite Eq. (1) in the form

$$-\varepsilon^2\phi^{\text{iv}}(x) + \phi''(x) + \Omega^2\phi = 0, \quad \Omega^2 = \rho\omega^2 L^2/\text{GA}. \tag{3}$$

This equation with attendant boundary conditions can be identified as a singular perturbation problem—on setting $\varepsilon = 0$, we obtain an equation of lower order which cannot satisfy all the required boundary conditions.

2. Asymptotic solution

For structures for which $\varepsilon \ll 1$, we expect that the mode shape should approximate solutions of

$$\phi''(x) + \Omega^2\phi = 0.$$

However, it is not clear which of the boundary conditions (Eq. (2)) are appropriate for this equation. Hence, let us represent the solution of Eq. (3) in the form of an asymptotic series given by

$$\phi(x,\varepsilon) = h_0(x) + \varepsilon h_1(x) + \varepsilon^2\, h_2(x) + O(\varepsilon^3). \tag{4}$$

where the dependency of the frequency on ε is taken in the form

$$\Omega^2 = \Omega_0^2(1 + \varepsilon\lambda_1 + \varepsilon^2\lambda_2 + O(\varepsilon^3)). \tag{5}$$

When these forms are substituted into Eq. (3), we obtain the following sequence of governing equations:

$$h_0''(x) + \Omega_0^2 h_0 = 0,$$
$$h_1''(x) + \Omega_0^2(h_1 + \lambda_1 h_0) = 0,$$
$$h_2''(x) + \Omega_0^2(h_2 + \lambda_1 h_1 + \lambda_2 h_0) - \Omega_0^4 h_0 = 0.$$

Solutions of these equations readily follow as

$$\begin{aligned} h_0(x) &= A_0 \sin \Omega_0 x + B_0 \cos \Omega_0 x, \\ h_1(x) &= A_1 \sin \Omega_0 x + B_1 \cos \Omega_0 x + x(\Omega_0\lambda_1/2)(A_0 \cos \Omega_0 x - B_0 \sin \Omega_0 x), \\ h_2(x) &= A_2 \sin \Omega_0 x + B_2 \cos \Omega_0 x + x(F_1 \sin \Omega_0 x + F_2 \cos \Omega_0 x), \\ &\quad - x^2(\lambda_1^2\Omega_0^2/8)(A_0 \sin \Omega_0 x + B_0 \cos \Omega_0 x), \end{aligned}$$

where

$$-2F_1/\Omega_0 = B_0(\lambda_2 - \Omega_0^2 - \lambda_1^2/4) + \lambda_1 B_1, \quad 2F_2/\Omega_0 = A_0(\lambda_2 - \Omega_0^2 - \lambda_1^2/4) + \lambda_1 A_1.$$

This solution is regarded as the "outer" solution, and is valid in a region away from the ends.

Following Refs. [2,3], we construct an "inner" solution near $x = 0$, expressed in terms of the coordinate $\tilde{x} = x/\varepsilon$, in the form

$$\phi(x,\varepsilon) = \varepsilon g_0(\tilde{x}) + \varepsilon^2 g_1(\tilde{x}) + O(\varepsilon^3). \tag{6}$$

When this form is substituted into Eq. (3), we find that both g_0, g_1 satisfy

$$g_i^{\text{iv}}(\tilde{x}) - g''(\tilde{x}) = 0 \quad (i = 0, 1),$$

with the boundary conditions that require

$$g_i(\tilde{x} = 0) = 0, \quad g_i'(\tilde{x} = 0) = 0 \quad (i = 0, 1).$$

It readily follows that

$$g_i(\tilde{x}) = C_i(\tilde{x} - 1 + \mathrm{e}^{-\tilde{x}}) \quad (i = 0, 1) \tag{7}$$

satisfy the boundary conditions and avoid exponential growth as $\tilde{x} \to \infty$.

The constants of integration that appear in the "inner" solution can be expressed in terms of those of the "outer" solution by means of applying the matching process in an intermediate layer. At this stage, we omit the details of the process as it is similar to that presented in Ref. [4]. In summary, the results include:

$$B_0 = 0, \quad C_0 = \Omega_0 A_0 = -B_1, \quad C_1 = \Omega_0(A_1 + \lambda_1 A_0/2) = -B_2. \tag{8}$$

Again, following Refs. [2,3], we construct an "inner" solution near $x = 1$, expressed in terms of the coordinate $x^+ = (x-1)/\varepsilon$, in the form

$$\phi(x,\varepsilon) = f_0(x^+) + \varepsilon f_1(x^+) + \varepsilon^2 f_2(x^+) + \varepsilon^3 f_3(x^+) + O(\varepsilon^4). \tag{9}$$

When this form is substituted into Eq. (3), we find that the functions $f_i(x^+)$ must satisfy

$$\begin{aligned} &f_i^{\mathrm{iv}}(x^+) - f_i''(x^+) = 0 \quad (i = 0, 1), \\ &f_2^{\mathrm{iv}}(x^+) - f_2''(x^+) = \Omega_0^2 f_0, \\ &f_3^{\mathrm{iv}}(x^+) - f_3''(x^+) = \Omega_0^2 (f_1 + \lambda_1 f_0), \end{aligned}$$

subject to the boundary conditions that

$$\begin{aligned} &f_i''(0) = 0, \\ &f_i'''(0) - f_i'(0) = 0. \end{aligned}$$

It readily follows that

$$\begin{aligned} &f_0 = D_0, \quad f_1 = D_1, \\ &f_2 = D_2 + \Omega_0^2 D_0 (\mathrm{e}^{x^+} - (x^+)^2/2), \\ &f_3 = D_3 + \Omega_0^2 (D_1 + \lambda_1 D_0)(\mathrm{e}^{x^+} - (x^+)^2/2), \end{aligned} \tag{10}$$

satisfy the boundary conditions and avoid exponential growth as $x^+ \to -\infty$.

The final determination of the unknown constants requires applying the matching process near $x = 1$. In summary, the results include

$$\begin{aligned} &\cos = \Omega_0 = 0, \quad \Omega_0 = (2n-1)\pi/2 \quad (n = 1, 2, 3, \ldots), \\ &\lambda_1 = 2, \quad \lambda_2 = 3 + \Omega_0^2, \\ &D_0 = A_0 \sin \Omega_0, \quad D_1 = A_1 \sin \Omega_0, \quad D_2 = (A_2 + \Omega_0^2 A_0/2) \sin \Omega_0. \end{aligned} \tag{11}$$

Finally, if we arbitrarily assign $\phi(x = 1, \varepsilon) = 1$, it follows that

$$f_0(x^+ = 0) = 1, \quad f_i(x^+ = 0) = 0, \quad (i = 1, 2, \ldots)$$

so we obtain

$$\begin{aligned} &D_0 = 1, \quad D_1 = 0, \quad D_2 = -\Omega_0^2, \\ &A_0 = \sin \Omega_0, \quad A_1 = 0, \quad A_2 = -(3\Omega_0^2/2) \sin \Omega_0, \\ &B_1 = B_2 = -\Omega_0 \sin \Omega_0. \end{aligned} \tag{12}$$

Table 1
Squared ratio of exact to predicted frequencies for the first three modes

α	$\left[\frac{\Omega^2(\text{exact})}{\Omega^2(3\text{-term})}\right]_{\text{mode-1}}$	$\left[\frac{\Omega^2(\text{exact})}{\Omega^2(3\text{-term})}\right]_{\text{mode-2}}$	$\left[\frac{\Omega^2(\text{exact})}{\Omega^2(3\text{-term})}\right]_{\text{mode-3}}$
10	1.001	0.9900	0.9767
15	1.002	0.9982	0.9932
20	1.002	0.9992	0.9990
25	1.000	1.001	0.9986
30	1.000	0.9994	1.001

3. Numerical results and discussion

As a measure of the accuracy of the asymptotic results, we compare the resulting frequencies and mode shapes with those obtained from the exact analysis [1]. It should be noted, however, that the process of obtaining numerical results from the exact analysis is difficult due to the presence of exponentially large terms.

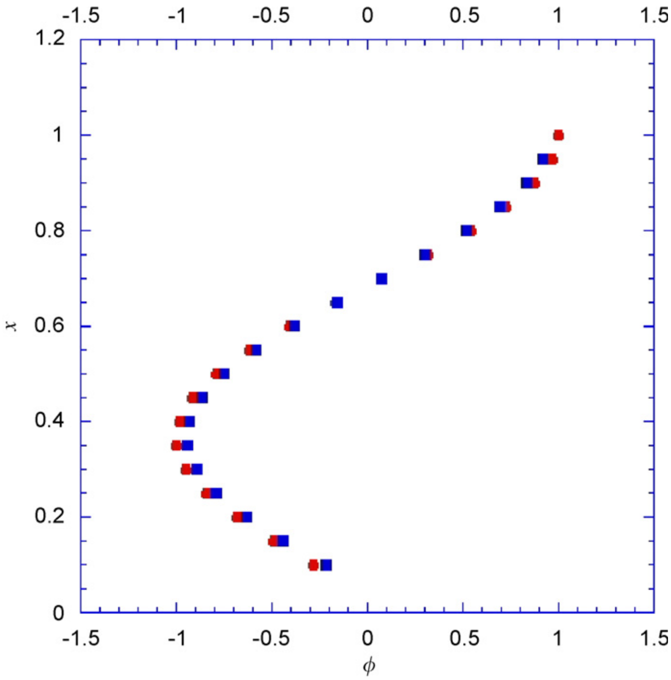

Fig. 1. Exact (●) and asymptotic (■) mode shapes for the second mode with $\alpha = 20$.

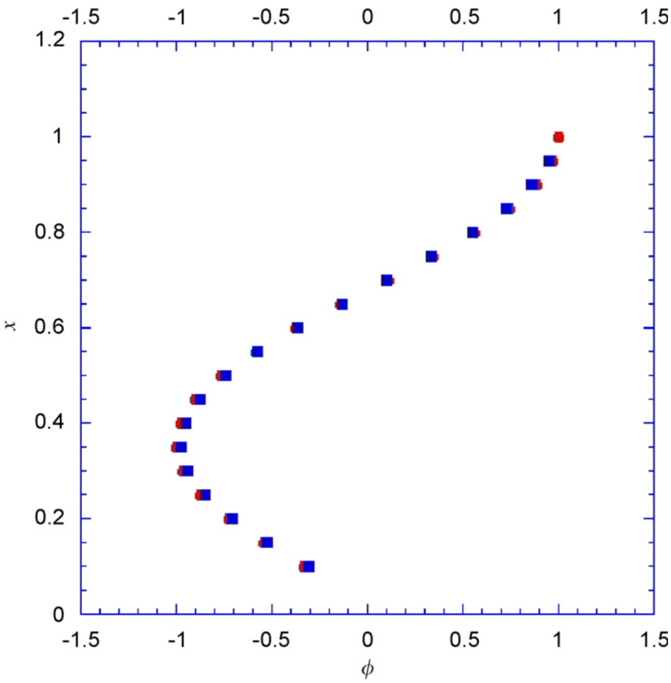

Fig. 2. Exact (●) and asymptotic (■) mode shapes for the second mode with $\alpha = 30$.

The calculated frequencies for the first three modes are given in Table 1 as a function of the stiffness parameter α. As can be seen, the frequencies obtained from the three-term asymptotic theory equation (5) approach those obtained from the exact analysis as the stiffness parameter increases. Further, the correspondence for moderate values of the stiffness parameter decreases as the mode number increases.

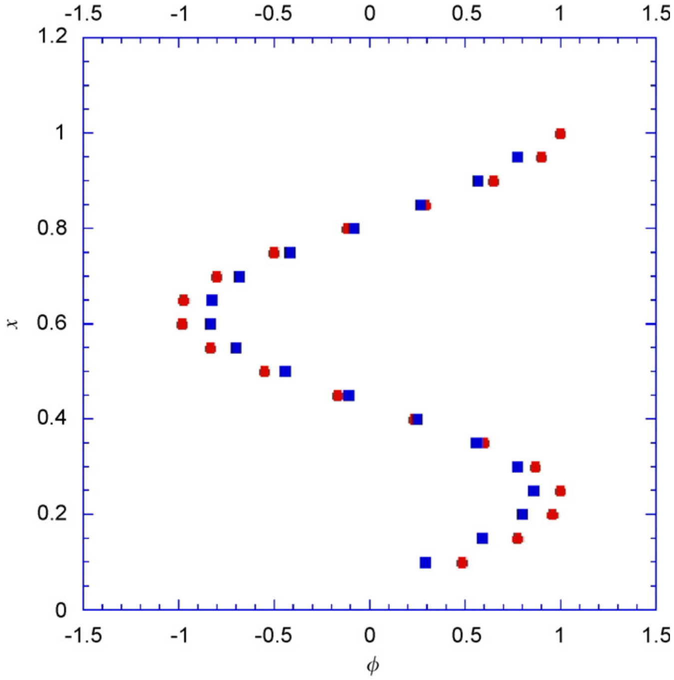

Fig. 3. Exact (●) and asymptotic (■) mode shapes for the third mode with $\alpha = 20$.

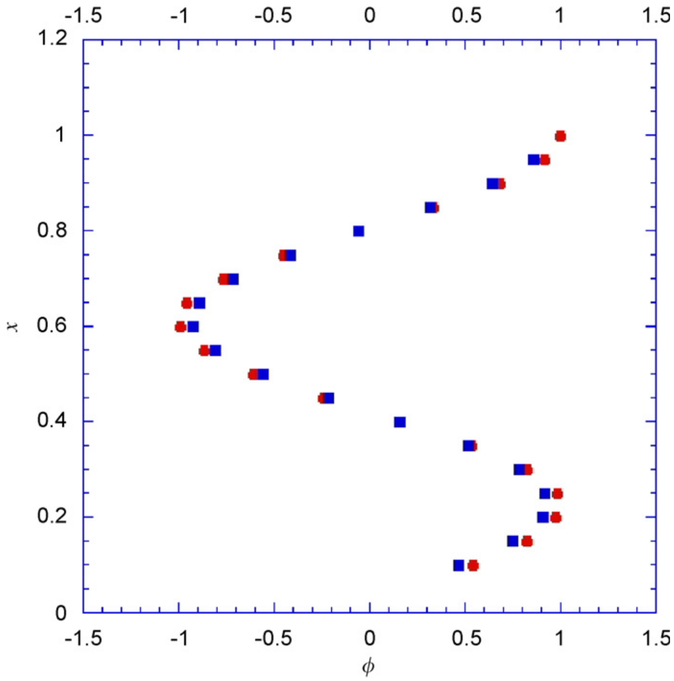

Fig. 4. Exact (●) and asymptotic (■) mode shapes for the third mode with $\alpha = 30$.

As the relative accuracy for frequency seems to be satisfactory for the higher values of the stiffness parameter, we present only the mode shapes for $\alpha = 20, 30$. Further, since the asymptotic results for the first mode are indistinguishable from the exact results, we present only the results for the second and third modes. It should also be noted that we only plot the outer solution component associated with the asymptotic solution as it is only in the immediate neighborhood of the end points that the inner solution is significant. The results for the second mode are presented in Figs. 1 and 2 and show that the nodes and the peaks occur at essentially the same place. The peak ordinates for $\alpha = 30$ seem to coincide whereas the peak ordinate for $\alpha = 20$ is slightly underestimated by the asymptotic theory. The results for the third mode presented in Figs. 3 and 4 again show that the nodes and peaks appear to coincide at the same point. However, the peak ordinates are underestimated by the asymptotic theory for both values of the stiffness parameter.

In summary, it has been found that the asymptotic results are a reasonable approximation to the exact results—particularly for large values $\alpha > 20$ of the stiffness parameter. Further, the general character of the motion is essentially that of a shear beam: the mode shape is a sine wave. The effects of the Euler–Bernoulli beam component is to introduce boundary layers near each end of the beam within which the boundary conditions adjust from the exact conditions to those of a shear beam. If we pick $\tilde{x} = 3$, $x^+ = -3$ as defining the essential width of the boundary layers, then this adjustment width is approximately $3\varepsilon L$.

References

[1] E. Miranda, S. Taghavi, Approximate floor acceleration demands in multistory buildings, I: formulation, *Journal of Structural Engineering* 131 (2005) 203–211.

[2] A.C. Heidebrecht, S. Smith, Approximate analysis of tall wall-frame structures, *Journal of Structural Division, ASCE* 99 (1973) 199–221.

[3] J. Kevorkian, J.D. Cole, *Perturbation Methods in Applied Mechanics*, Springer, New York, 1981.

[4] H.E. Williams, A singular perturbation solution for the beam-string, *Journal of Sound and Vibration* 120 (1988) 631–632.

[5] E.E. Traum, W.P. Zalewski, An analogy to the structural behavior of shear-wall systems, *Journal of Boston Society Civil Engineers* 57 (1970) 303–335.